# Direct observation of internal energy distributions of C5−

M. Goto, A. E. K. Sundén, H. Shiromaru, J. Matsumoto, H. Tanuma et al.

Citation: J. Chem. Phys. **139**, 054306 (2013); doi: 10.1063/1.4817196
View online: http://dx.doi.org/10.1063/1.4817196
View Table of Contents: http://jcp.aip.org/resource/1/JCPSA6/v139/i5
Published by the AIP Publishing LLC.

# Direct observation of internal energy distributions of $C_5^-$

M. Goto,[1] A. E. K. Sundén,[1] H. Shiromaru,[2] J. Matsumoto,[2] H. Tanuma,[3] T. Azuma,[4] and K. Hansen[1]

[1]*Department of Physics, University of Gothenburg, 41296 Gothenburg, Sweden*
[2]*Department of Chemistry, Tokyo Metropolitan University, 1-1 Minamiosawa, Hachiouji-shi, Tokyo 192-0397, Japan*
[3]*Department of Physics, Tokyo Metropolitan University, 1-1 Minamiosawa, Hachiouji-shi, Tokyo 192-0397, Japan*
[4]*Atomic, Molecular and Optical Physics Laboratory, RIKEN, 2-1, Hirosawa, Wako-shi, Saitama 351-0198, Japan*

(Received 21 March 2013; accepted 17 July 2013; published online 6 August 2013)

Photon induced decay of $C_5^-$ has been measured in an electrostatic storage ring. The time dependence of the photo-enhanced decay is close to a $1/t$ decay which indicates a thermal process. The deviation from the expected power of $-1$ is quantitatively explained by the small heat capacity of the anion. Measurements of the photo-enhanced decay at different storage times and photon energies allow a determination of the radiative cooling rate and the energy distribution of the ions. The average energy content between 15 and 70 ms is found to vary as time to the power $-0.72$, and at 50 ms the ions contain an average excitation energy of 0.5 eV. The time dependent energy distribution is consistent with cooling by infrared photon emission if published oscillator strengths are reduced by a factor 2.5, in contrast to cooling of larger molecular carbon-based ions where electronic transitions cause a much stronger cooling. © *2013 AIP Publishing LLC*. [http://dx.doi.org/10.1063/1.4817196]

## INTRODUCTION

Carbon clusters occur naturally with sizes from a few atoms to the fullerenes that have been observed both in space[1] and in the laboratory.[2,3] Fullerenes are known to lose excitation energy thermally by thermionic emission,[4] evaporation of small neutral fragments,[5] and by emission of radiation,[6,7] and by now all three decay channels are well established, both with respect to the thermal nature of the processes and also to a large extent to the values of the parameters that characterize them, such as activation energies[8] and radiative cooling rates.[6,9]

Much less is known about the cooling of smaller carbon clusters. The stabilizing effect of radiative cooling has important implications for the survival and abundance of carbon containing molecules and ions in interstellar space,[10] and for astrophysical applications it is therefore important to determine the systematics of radiative cooling rates of these species.

One of the surprising features of fullerene radiative cooling was the strong enhancement of the emitted power compared to the power deduced from the vibrational oscillator strengths.[6,7,9] The origin of this enhancement, which is typically two orders of magnitude for anions and even more for the cations, was identified as an effect of the surface plasmon resonance. This resonance accounts for a large fraction of the total oscillator strength and with its large width it reaches down to very low energies. This behavior has been described with a classical model in Ref. 11 and found to agree well with experimentally measured cooling rates for the range of fullerene anions studied in Ref. 12.

Also smaller molecules may have strongly elevated cooling rates. In a recent study of cations of the smaller molecule anthracene, $C_{14}H_{10}$, the radiative cooling was found to be strongly enhanced, an effect ascribed to photon emission from a thermally excited electronic states.[13] Given that the plasmon resonance can be constructed out of particle-hole excitations, this mechanism carries strong analogies to fullerene cooling. An obvious question is then if small carbon clusters cool similarly to larger carbon containing molecules or not.

Here, we report the observation of time resolved electron emission from $C_5^-$ anions on the time scale of tens of microsecond after laser excitation. The characteristic time profile of the decay allows us to conclude that the process is thermal. Furthermore, the well defined amount of energy imparted into the cluster by the photon in the excitation process, together with the strong energy dependence of the emission constant, selects a specific and, by virtue of the small heat capacity of $C_5^-$, very narrow internal excitation energy for the anions that decay in the observed time interval. By variation of the laser excitation time, this permits measurements of the internal energy distribution of the ions and its time development.

## EXPERIMENTAL PROCEDURE

The experiments were performed with an electrostatic storage ring that can store ions up to several seconds, although storage times were restricted to below 100 ms in the present experiments. The carbon cluster anions were produced from a graphite disk in a laser ablation source operated without any cooling gas. The ablation laser was a Nd:YAG laser with a wavelength of 532 nm and a pulse duration of several ns. The ions were extracted by a pulsed field, accelerated to 15 keV and injected into the ring. The $C_5^-$ ions of $m/q = 60$ u/$e$ had a

 

revolution time of 35.3 $\mu$s in the ring and were selected by applying kick-out pulses to the co-accelerated unwanted cluster masses at the storage times of 0.02 and 0.3 ms, with the procedure described in Ref. 14. The procedure eliminated masses that differ by 1 Da and the selection of an ion composed exclusively of $^{12}$C atoms ruled out any contamination with hydrogenated species. The neutral decay products were detected as function of the storage time with a microchannel plate located at the end of the straight section of the ring opposite to the side used for the laser excitation. The photo-enhanced neutralization decay was thus measured at times corresponding to 1/2, 3/2, 5/2, etc., turns, or 17.7 $\mu$s, 53.0 $\mu$s, 88.4 $\mu$s, etc., after photon absorption. Note that the quantity measured in these experiments is the decay *rate* and not a rate *constant*. More details on the storage ring can be found in Refs. 14 and 15.

The excitation photons were provided by a tunable nanosecond laser with a pulse duration of few ns. The laser was used with the wavelengths 480, 520, 610, 660 nm. The light was unfocused and pulse energies were kept at or below 3.5 mJ where the enhancement vs. fluence is linear, ensuring single photon absorption conditions.[16]

The branching between electron emission and emission of a heavy fragment is strongly in favor of the former in the present experiments. This conclusion is reached by comparing the two relevant activation energies. The lowest energy channel for dissociation is the loss of a neutral atom for which the activation energy is 4.9 eV as calculated with Born-Haber cycles and data from Refs. 17 and 18. This should be compared with the electron affinity of 2.85 eV. Experiments with 4.03 eV photons[19] also yield electron detachment exclusively for this cluster size, although the photon energy makes it possible that this may be a direct detachment process.

The decay curves recorded without exposing the ions to the laser pulse consist of two different regimes. The first is dominated by the spontaneous decay of the ions induced by the excitation energy acquired in the source during production. The decay is non-exponential, decreases rapidly, and has essentially vanished 4-6 ms after injection. The non-exponential time dependence is a consequence of the width of the internal energy distribution and is expected from other studies.[21] The second part of the spectra is almost constant and is generated by collisions of cluster ions and rest gas molecules. A single lifetime slightly above 1 s could be fitted to this weak component which should be compared with the 100 ms injection cycle of the ions into the ring. An example of a spectrum is shown in Figure 1. It includes a photo-enhanced signal seen as a sharp peak around 30 ms. The spacing between the peaks in the inset corresponds to the circulation time for the ions in the ring.

The photo-enhanced signal is extracted from the total signal after subtraction of the spontaneous, mainly collision induced decay by reference spectra recorded without laser excitation, and normalization of the subtracted spectrum to the source intensity and to the part of the beam exposed to the laser. The ion bunches spread out in the ring with time in a manner consistent with a spread in kinetic energy from the source of a few eV, and the ion concentration is obtained by multiplication of the yield by this experimentally determined

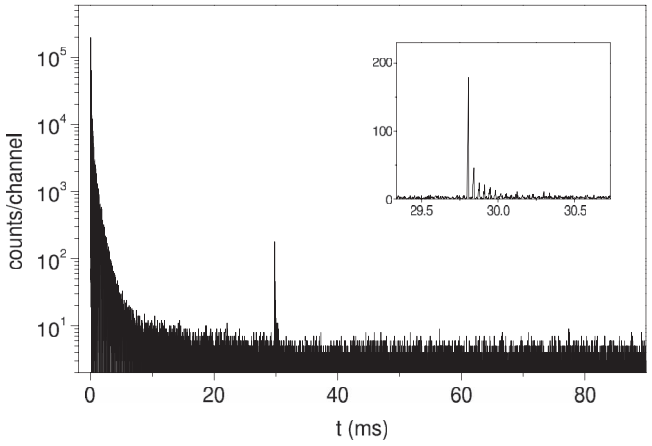


FIG. 1. A neutralization spectrum where the laser was fired at 30 ms with $\lambda = 480$ nm. The inset shows an expanded view around the laser firing time.

width. The net result of the normalization procedure is a signal which is normalized to all experimental factors except the overlap between the ion and laser beams and the related problem of betatron oscillations.

## DECAY OF THE PHOTO-ENHANCED SIGNAL

The photo-enhanced neutralization yield will first be analyzed with respect to the time dependence of the signal after laser excitation. Figure 2 shows the photo-enhanced neutralization signal for the first ten turns after the laser pulse. Two experimental averages and three theoretical curves are shown. The experimental curves are expected to be powerlaws on general grounds,[21] with a power close to $-1$. The power will, however, be slightly modified by any slope present in the energy distribution.[20] Decays originating from a decreasing part of an energy distribution will have a power which is numerically slightly smaller and vice versa for the power from an

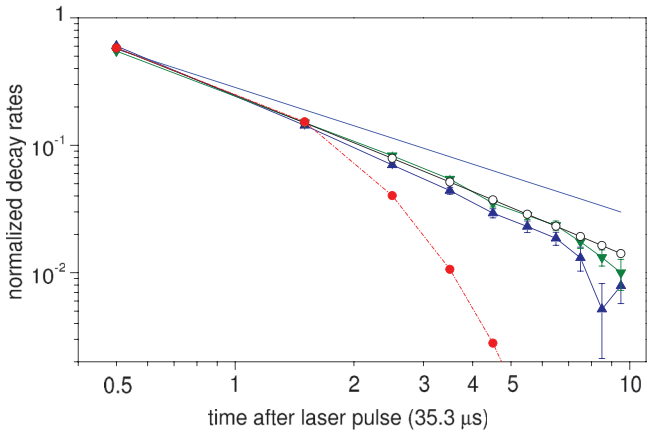


FIG. 2. The time dependence of the photo-enhanced decay. The experimental signals are normalized so the ten turns sum to unity. The triangles pointing up and down are the averages of enhancements measured at laser firing times before and after the peak signal time in Figure 3, respectively. The open circles are simulated points, assuming a flat excitation energy distribution, and the solid blue line is the $1/t$ decay. The filled circles is an example of an exponential, in this case with a rate constant of $3.8 \times 10^4$ s$^{-1}$. No physical significance should be attached to this value.

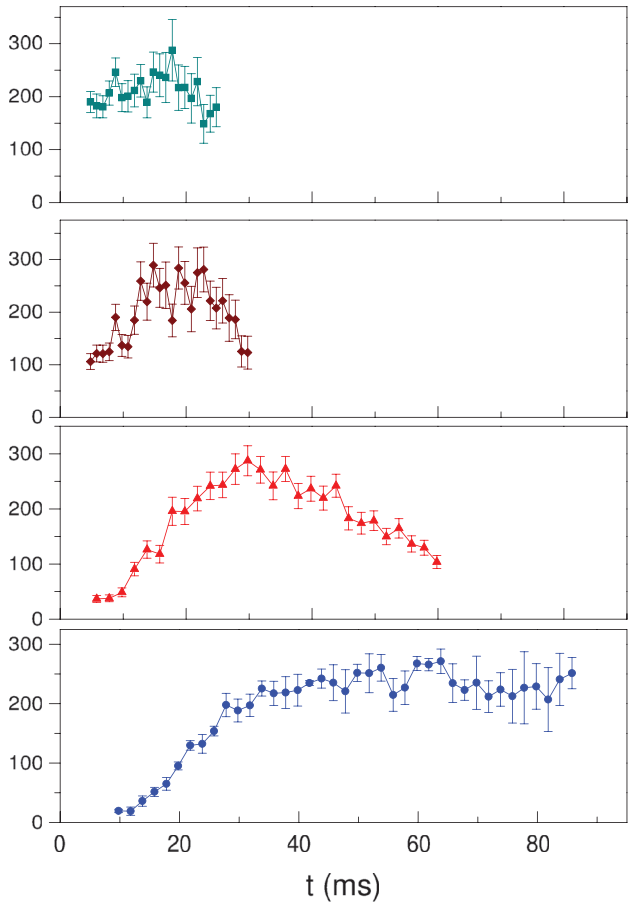


FIG. 3. The photo-enhanced signal vs. laser firing time. (Top to bottom) $\lambda = 660$, 610, 520, and 480 nm ($h\nu = 1.88$, 2.03, 2.38, and 2.58 eV). The uncertainties are $1-\sigma$ values, based on reproducibility. The amplitude has been normalized to the same maximum value.

increasing part of the distribution. It is therefore of interest to compare slopes from increasing and decreasing parts of the distribution. This is accomplished by comparing the measured enhancement curves from two groups; one where the laser has been fired before the peak intensity in the enhancements in Figure 3, and one where the laser was fired after. The two experimental curves include data for all wavelengths to improve statistics (the decay of the photo-enhanced signal, turn-by-turn after the laser pulse, showed no significant differences for different wavelengths, although the overall neutralization yield (the amplitude of the decay curve) was of course wavelength dependent). Both curves are well represented by powerlaw decays up to and including turn number seven. The deviations at turns 8 through 10 can tentatively be ascribed to radiative cooling. The good fit to a powerlaw decay proves that the decay involves a continuum of decay constants in the ensemble,[21,22] and the most likely candidate is a thermal distribution with sufficient width.

The powers from the two parts of the spectra are similar, albeit not identical, $-1.24 \pm 0.03$ and $-1.38 \pm 0.02$. These values bracket the value for a (hypothetical) flat internal energy distribution. Although we will show below that the energy distributions is not globally flat, the effect of this on the measured powers is seen to be small and we can use the measured powers to draw conclusions about the nature of the decay. To wit: the value for a flat distribution is a property of the ion and depends only on its electron emission rate constant and, very weakly, on the measurement time scale. The value for ions with large heat capacities is expected to be close to $-1$ on fairly general grounds.[20] Deviations from this value arise predominantly from the finite heat capacity of the ion and should be reproduced by the correct microscopic theory for electron emission from $C_5^-$. It thus constitutes a check of the description of the thermionic emission process, independent of effects due to the energy distribution that would otherwise complicate the comparison.

To calculate the corrections to the power of $-1$ and to describe the competition of electron emission and radiative cooling, the expression for the electron emission rate constant will now be calculated. The detailed balance equation is, for a given excitation energy $E$ and electron kinetic energy $\varepsilon$,[23] equal to

$$k(E,\varepsilon)d\varepsilon = \frac{2m_e}{\pi^2\hbar^3}\varepsilon\sigma_c(\varepsilon)\frac{\rho_{C_5}(E-E_a-\varepsilon)}{\rho_{C_5^-}(E)}d\varepsilon, \qquad (1)$$

where $m_e$ is the mass of the electron, $\rho_{C_5}$ and $\rho_{C_5^-}$ the level densities of the neutral and the anion, respectively, including the electronic degeneracies of 1 and 4 for $C_5$ and $C_5^-$, respectively. The spin degeneracy for the emitted electron is included explicitly. $E_a$ is the electron emission activation energy, and $\sigma_c$ is the electron capture cross section by the neutral cluster.

The electron kinetic energy is not observed in these experiments and can be integrated out after the neutral molecule level density and the capture cross section have been determined. The vibrational level densities were calculated with the Beyer-Swinehart algorithm and the frequencies (in $cm^{-1}$) 1828, 1807, 1399, 738, 714, 575, 411, 343, 162, 159, for the anion,[24] scaled with a factor 0.95, as recommended, and 1988, 779, 2169.44, 1446.6, 218, 216, 535, 535, 118, 118 for the neutral.[17,25–29] These frequencies refer to the electronic ground state which is calculated to be linear, consistent with both ion mobility[30] and UPS studies[31] where ions up to size $n = 9$ were found to be linear. The activation energy $E_a$ in Eq. (1) was assumed to be the vertical electron affinity of 2.853 eV.[32]

The capture cross section of the electron and neutral is calculated as the Langevin cross section,

$$\sigma = \left(\frac{2\alpha}{\varepsilon}\right)^{1/2}, \qquad (2)$$

where $\alpha$ is the polarizability of $C_5$. The geometry-averaged value of 71.7 a.u. was used[33] which gives

$$\sigma = 38.9\,[\text{Å}^2]\left(\frac{[\text{eV}]}{\varepsilon}\right)^{1/2}. \qquad (3)$$

The kinetic energy is fairly small and this cross section is significantly larger than the one corresponding to a geometric cross section, for example.

The kinetic energy integrated yield calculated with this rate constant for the experimental time window is shown in Figure 2 as open circles. The calculated signal is found to be very well represented by a powerlaw decay proportional to $t^{-1.26}$. This is a slightly steeper decrease than calculated from

the leading order correction to the $1/t$ decay, $-1 - 1/(C - 1) = -1.21$,[21] where $C$ is taken to be the canonical heat capacity (in units of $k_B$) of the neutral molecule at the temperature corresponding to the relevant excitation energy (shown below to be equal to 2.95 eV$-E_a$). The value $-1.26$ only changes to $-1.28$ if the rate constant is arbitrarily increased by a factor of three, indicating a rather weak dependence on the electron emission rate constant frequency factor. We conclude that the time dependence of the photo-enhanced signal agrees fairly well with the theoretically expected. This contrasts with results on small aluminium anions ($Al_4^-$ and $Al_5^-$)[34] where the deviation of the power from $-1$ is significantly larger.

The conclusion that the photo-enhanced electron emission is thermal differs from the interpretations of previous measurements of spontaneous decay of small odd-numbered anion carbon clusters and $C_2^-$.[35] These decays, on time scales below 10 ms, were ascribed to long-lived excited electronic states, with the argument that the energy content of the anions would not allow a thermal emission of an electron. The laser excitation technique applied here allows detection on much shorter time scales and supports an interpretation in terms of thermal decay for those experiments also. The spontaneous decay $C_2^-$ differs in this respect, but can readily be explained with the mechanism given in Ref. 22.

A similar observation can be made concerning the measurements in an electrostatic trap of photon-induced decay yields of $C_5^-$.[36] The ions were exposed to photons of energies 1.2 and 2.3 eV, and the neutralization yields were observed to decrease rapidly with storage time, and were fitted with a single lifetime of 18 ms. The authors discuss the decay in terms of a low lying isomer and vibrational radiative cooling, but find the latter unlikely.

## COOLING RATES AND ENERGY DISTRIBUTIONS

We now turn to the variation of the neutralization signal over longer times. The normalized signal summed over the first two turns after the laser pulse is used as the photo-enhanced signal in the analysis. It is shown in Figure 3.

From the observation that the yield changes with the laser firing time, we conclude that the ions cool radiatively, at least after 4-6 ms where the spontaneous decay has terminated, because the energy distributions do not change by depletion after this time, and the only possible cooling channel is then radiative cooling. A simple interpretation of the curves in Figure 3 is then that they represent the internal energy distributions of the ions. The fact that the signal, for a given photon energy, increases at short times to a maximum and decreases again at longer times therefore provides information about the details of this distribution and how it varies with time, i.e., the cooling rates.

The key observation that allows one to extract energy distributions from the measured yields is that the electron emission rate constant increases rapidly with the excitation energy due to the small heat capacity of the clusters. This effectively restricts the energy of the anions that neutralize in the experimental time window to a very narrow energy interval (see Ref. 37 for a demonstration of this for $C_N^-$, with $N = 14$, 18, 22 and Ref. 38 for zinc phthalocyanine).

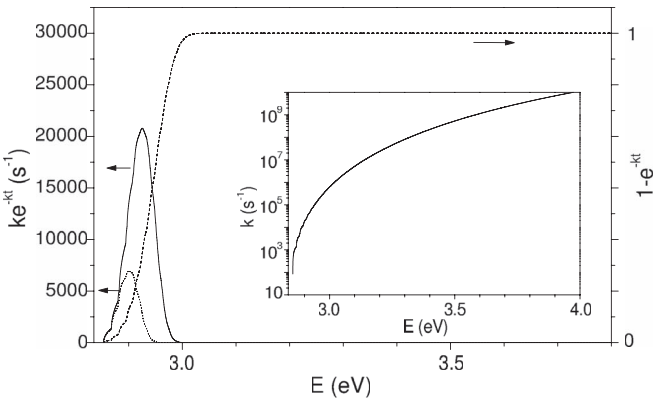


FIG. 4. The electron detachment rates vs. internal energy calculated for 17.7 $\mu$s (solid curve) and 53.1 $\mu$s (dotted curve) after photo-excitation, showing the neutralization yields at the first and the second peaks. The dashed line is the probability of decay before 6 $\mu$s, approximately the residence time in the first straight section immediately after laser excitation. The inset shows the calculated electron emission rate constant.

In our case, the narrow energy band is only slightly above the electron affinity, which is of course the absolute threshold for emission. The distribution of energies of the anions that decay at a given time $t$ is given by $g(E)k(E)\exp(-k(E)t)$, where $g(E)$ is the density of ions with energy $E$, and $k(E)$ the electron emission rate constant. A numerical evaluation of this energy distribution, setting $g$ constant and $t = 17.7$ $\mu$s, which corresponds to the first observed photo-enhanced peak, gives an approximately gaussian shape centered at 2.95 eV and a full width at half maximum of 0.08 eV. We will denote this "magic energy" of 2.95 eV by $E_0$. For decay at the second turn after photoexcitation, the value is reduced by 0.03 eV. Because this change is so much smaller than both the photon energy and $E_0 - h\nu$, we will take $E_0$ to be constant in the analysis below. The situation is illustrated in Figure 4. It is worth pointing out that excitation energies of twice the lowest photon energy give rise to decays at time scales significantly below the shortest resolvable ones in these experiments. The possibility of multiphoton absorption processes is therefore irrelevant for the interpretation of our data.

With a well defined $E_0$ the measured photo-enhanced signal, $I$, will be given by

$$I(h\nu, t_{las}) \propto \sigma(h\nu) g(E_0 - h\nu, t_{las}), \tag{4}$$

where $t_{las}$ is the laser firing time, $\sigma$ is the photon absorption cross section, and $g$ the excitation energy density of the anion. The constant of proportionality is related to the detection efficiency and is universal due to our signal normalization procedure. A schematic view of the two-dimensional map of the energy distribution undergoing radiative cooling is shown in Figure 5.

The yields vs. time were found to scale with time which made it possible to place all the measured data on a single curve, as shown in Figure 6. The scale factors are $s = 2.84 \pm 0.37$, $2.02 \pm 0.22$, $1.10 \pm 0.05$, $0.625 \pm 0.03$ for the photon wavelengths 660, 610, 520, and 480 nm. The fit function used was $A \cdot \exp(0.33944\tau - 0.01026\tau^2 + 0.00013\tau^3 - 6.208 \times 10^{-7}\tau^4)$, with $\tau \equiv st_{las}$. No significance should be attached to the specific functional form.

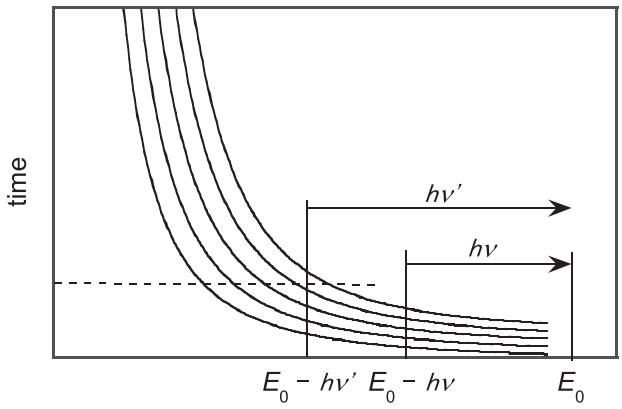


FIG. 5. A schematic rendition of the measured distributions and their relation to $E_0$. The vertical lines give the direction of the measurements for two different photon energies in the experiments. The energy distribution for a given time corresponds to a cut parallel to the abscissa, illustrated with a horizontal line. The curved lines illustrate schematically the motion with time of constant (relative) densities of the distribution. As discussed in the text, it should not be inferred that ions cool along these trajectories.

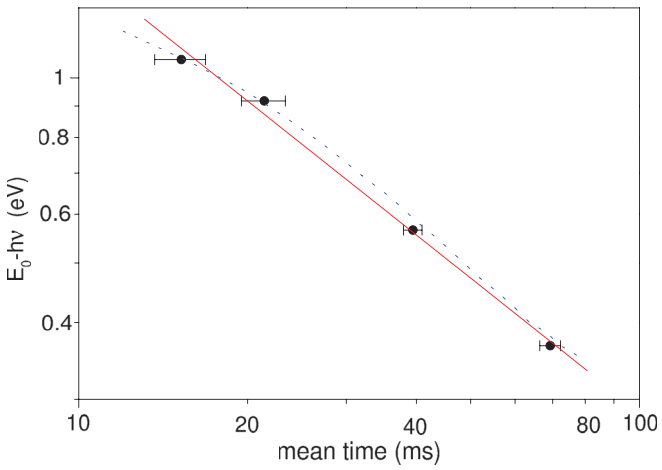


FIG. 7. The sampled energy $E_0 - h\nu$ vs. the mean time of the yield distribution. The full line is a straight line fit with the slope $-0.72 \pm 0.04$. The dashed curve is the mean energy calculated in the simulations described below.

The good scaling shows that the average times and the widths of the yield curves are proportional. They can be found from the mean and standard deviation of the fit function, $\langle\tau\rangle = 43.34$, $\sigma_\tau = 19.61$. A plot of the energy $E_0 - h\nu$ vs. the average of the time in the distributions in Figure 3 is shown in Figure 7. The dependence is consistent with an inverse powerlaw in time, with a fitted power of $-0.72 \pm 0.04$

$$E_0 - h\nu = 8.0\,[\mathrm{eV(ms)}^{0.72}]\bar{t}^{\,-0.72}, \tag{5}$$

where $\bar{t} = <\tau>/s$. The scaling parameter $s$ therefore depends on the anion energy $E$ as

$$E \propto s^{\delta}, \tag{6}$$

with the definition $\delta \equiv 0.72$.

The measured data do not give the energy distributions directly, but the scaling allows to express the distribution in terms of energy instead of time. Because the energy and the scaling parameter are related by Eq. (6), we can drop the energy argument in the distribution $g$ and use the relation between energies and observation times as follows:

$$t_{las} s_2 = t_{ref} s_1, \tag{7}$$

where $t_{ref}$ is an arbitrary chosen reference time and the values of $s_1$, $s_2$ are related to energies by Eq. (6), $s_2 \propto (E_0 - h\nu)^{1/\delta}$ and the variable in the energy distribution is $s_1 \propto E^{1/\delta}$. This gives

$$E = (E_0 - h\nu)\left(\frac{t_{las}}{t_{ref}}\right)^{\delta}. \tag{8}$$

The scaling properties of the distributions imply that

$$s_1 g(t_{ref}) = s_2 g(t_{las}), \tag{9}$$

which gives

$$g(t_{ref}) = \frac{t_{las}}{t_{ref}} g(t_{las}) \propto \frac{t_{las}}{t_{ref}} I(t_{las}), \tag{10}$$

at the energy given in Eq. (8). The constant of proportionality in Eq. (10) is independent of the laser firing time. The result of this conversion is shown in Figure 8 which gives the energy distribution vs. the absolute energy for $t_{ref} = 50$ ms.

Instead of the above interpretation one could postulate a metastable electronic excited state which could contribute a long time component of the photo-enhanced decay. In the simplest case involving a single excited state, the photo-enhanced signal would be given by

$$I(h\nu, t_{las}) \propto a_0 e^{-t/\tau} + a_1(1 - e^{-t/\tau}), \tag{11}$$

where $\tau$ is the lifetime of the excited state and the coefficients $a_0$, $a_1$ are related to the photoabsorption cross section and the initial populations. Obviously, this expression does not reproduce the time dependence observed for even a single wavelength. Addition of another hypothetical electronically excited state as an intermediate state could in principle give a yield curve that would increase with time, peaks and decrease again. To reproduce the behavior in Figure 3 would however require at least four different intermediate states with different

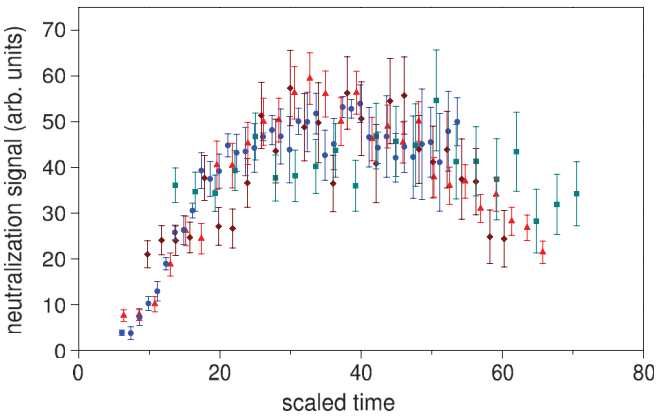


FIG. 6. Neutralization yields with the time axis scaled with a constant factor for each photon energy. The symbols for photon wavelengths are the same as used in Figure 3. A few points below 4 ms are excluded here and in the following to avoid complications from spontaneous electron emission.

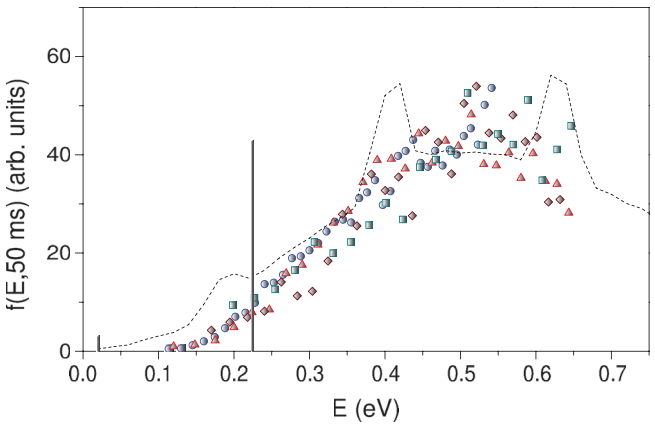


FIG. 8. The energy distributions for all photon energies, scaled to 50 ms. The symbols are used as in Figure 6. The dashed line is the distribution calculated with the simulations described in the text. The two vertical sticks give the photon energy of the IR active modes, with the height indicating the relative oscillator strength.

lifetimes, one for each wavelength. This is logically possible but highly unlikely and we will not consider the possibility further.

## COOLING MECHANISM

The stochastic nature of the energy emission plays a role in shaping the observed energy distributions. This can be seen immediately from the curves in Figure 3. If the radiative cooling were to proceed via emission of a high number of photons of sufficiently low energy, it could be considered continuous and deterministic in the sense that an anion excitation energy would be completely determined at a later time from the initial energy. Such a deterministic development implies that ions with specific internal energies would follow identical trajectories in the $(E, t)$ space, apart from a constant displacement in time. This would imply that the measurements with different photon energies in Figure 3 would have the same width in time as those at any other photon energy. This is obviously not the case experimentally, and we conclude that the stochastic elements in the decay are causing observable effects in the energy distributions. The energies of the photons emitted from the anions therefore constitute a large fraction of the total excitation energy of the anions and consequently only a few photons are emitted.

We have compared the observed distributions with the energy distributions generated with a simulation based on the IR oscillator strengths from the literature.[24] The highest oscillator strength transition ($f_1 = 855$ km/mol, for $\hbar\omega_1 = 1807$ cm$^{-1}$) was included together with two close-lying lines in the low energy part of the spectrum. The small splitting between these two allows us to treat them as one line at 160 cm$^{-1}$ with intensity $f_2 = 59$ km/mol. One other IR active transition is high in energy and has little oscillator strength, and has for simplicity been left out of the analysis.

When two IR modes in the harmonic approximation contributes to emission of radiation, the photon emission rate constant is ($\rho(E < 0) = 0$)

$$k_{ph} = \sigma_1 \frac{8\pi\nu_1^3}{c^2} \frac{1}{\rho(E)} \sum_{n=0}^{\infty} n\rho^{(1)}(E - nh\nu_1) + \sigma_2 \frac{8\pi\nu_2^3}{c^2} \frac{1}{\rho(E)} \sum_{n=0}^{\infty} n\rho^{(2)}(E - nh\nu_2), \quad (12)$$

where the superscript indicates that the emitting mode has been excluded from the level density, the level density $\rho(E)$ is calculated including all modes, and the IR photon absorption cross sections $\sigma_i$ $(i = 1, 2)$ are given by $f_i c \ln(10)/N_A \nu_i$, where $N_A$ is Avogadro's number. For high temperatures, the terms involving level densities reduce to $\exp(-h\nu/T)/(1 - \exp(-h\nu/T))$, as expected.

The simulations followed photon emission processes of $10^4$ decay chains, starting at anion energies selected randomly in an energy interval with a width of 1 eV. All three level densities were smeared over 5 cm$^{-1}$ to mimic the rotational effects not accounted for in Eq. (12).

In the energy interval corresponding to the observed (0.37 eV–1.07 eV), the simulated mean energy decreased with a powerlaw in time and saturated at 0.27 eV at long times. The power in the powerlaw decay depended on the initial energy and was found to reproduce the experimental value $-0.72$ for initial energies in the interval 2 eV $\pm$ 0.5 eV. The time scale, however, was a factor of 2.5 shorter than the experimentally observed, indicating oscillator strengths that are smaller than the calculated by this factor. The factor is virtually unchanged if the level density is not smoothened, the only difference being a higher asymptotic energy and a less smooth final distribution.

The simulated mean energies are plotted as a dashed curve in Figure 7 with this scaling. The energy distribution at 20 ms was also calculated, with a statistics of $2 \times 10^7$ and is shown in Figure 8, after scaling to 50 ms. Although not perfect, the agreement between measured and simulated data is nevertheless satisfactory. The structure in the curve is due to the simplifying assumptions made in the simulations where broadening effects on the emission line due to the high temperatures have been ignored.

We conclude that the energy distributions can be reproduced with the few IR active modes provided the oscillator strengths are reduced by a factor of 2.5, and the initial excitation energy generated in the laser ablation is around 2 eV.

## SUMMARY

The photon induced electron emission of $C_5^-$ has been measured in an electrostatic storage ring and found to be thermal. The neutralization yield were found to vary with laser firing time which can be understood in terms of radiative cooling. Internal energy distributions could be extracted from the experimental data and comparison of data obtained with different photon energies gave consistent distributions. The radiative cooling is accounted for by the vibrational infrared photon emission. This contrasts with data known for fullerenes and other large carbon containing molecules and

suggests a size dependent cooling mechanism for carbon containing molecules.

## ACKNOWLEDGMENTS

This work has been supported by the Department of Physics at the University of Gothenburg, the Swedish Foundation for International Cooperation in Research and Higher Education (STINT), and the Japanese Society for Promotion of Science.

[1] J. Cami, J. Bernard-Salas, E. Peeters, and S. E. Malek, Science **329**, 1180 (2010).
[2] H. W. Kroto, J. R. Heath, S. C. O'Brien, R. F. Curl, and R. E. Smalley, Nature (London) **318**, 162 (1985).
[3] W. Krätschmer, L. D. Lamb, K. Fostiropoulos, and D. R. Huffman, Nature (London) **347**, 354 (1990).
[4] E. E. B. Campbell, G. Ulmer, and I. V. Hertel, Phys. Rev. Lett. **67**, 1986 (1991).
[5] S. C. O'Brien, J. R. Heath, R. F. Curl, and R. E. Smalley, J. Chem. Phys. **88**, 220 (1988).
[6] K. Hansen and E. E. B. Campbell, J. Chem. Phys. **104**, 5012 (1996).
[7] A. E. K. Sundén, M. Goto, J. Matsumoto, H. Shiromaru, H. Tanuma, T. Azuma, J. U. Andersen, S. E. Canton, and K. Hansen, Phys. Rev. Lett. **103**, 143001 (2009).
[8] K. Hansen and O. Echt, Phys. Rev. Lett. **78**, 2337 (1997).
[9] J. U. Andersen, C. Brink, P. Hvelplund, M. O. Larsson, B. Bech Nielsen, and H. Shen, Phys. Rev. Lett. **77**, 3991 (1996).
[10] C. Joblin, P. Boissel, and P. de Parseval, Planet Space Sci. **45**, 1539 (1997).
[11] J. U. Andersen and E. Bonderup, Eur. Phys. J. D **11**, 413 (2000).
[12] J. U. Andersen, C. Gottrup, K. Hansen, P. Hvelplund, and M. O. Larsson, Eur. Phys. J. D **17**, 189 (2001).
[13] S. Martin, J. Bernard, R. Brédy, B. Concina, C. Joblin, M. Ji, C. Ortega, and L. Chen, Phys. Rev. Lett. **110**, 063003 (2013).
[14] S. Jinno, T. Takao, K. Hanada, M. Goto, K. Okuno, H. Tanuma, T. Azuma, and H. Shiromaru, Nucl. Instrum. Methods Phys. Res. A **572**, 568 (2007).
[15] M. Goto, M. Togawa, S. Jinno, T. Takao, J. Matsumoto, H. Shiromaru, Y. Achiba, H. Tanuma, and T. Azuma, Chem. Phys. Lett. **460**, 46 (2008).
[16] M. Ohara, H. Shiromaru, Y. Achiba, K. Aoki, K. Hashimoto, and S. Ikuta, J. Chem. Phys. **103**, 10393 (1995).
[17] A. van Orden and R. J. Saykally, Chem. Rev. **98**, 2313 (1998).
[18] NIST Chemistry WebBook, NIST Standard Reference Database Number 69, edited by P. J. Linstrom and W. G. Mallard (National Institute of Standards and Technology, Gaithersburg, MD, 2013), see http://webbook.nist.gov (retrieved January 22, 2013).
[19] B. Pozniak and R. C. Dunbar, Int. J. Mass Spectrom. Ion Process. **133**, 97 (1994).
[20] K. Hansen, *Statistical Physics of Nanoparticles in the Gas Phase* (Springer, Netherlands, 2013).
[21] K. Hansen, J. U. Andersen, P. Hvelplund, S. P. Møller, U. V. Pedersen, and V. V. Petrunin, Phys. Rev. Lett. **87**, 123401 (2001).
[22] J. Fedor, K. Hansen, J. U. Andersen, and P. Hvelplund, Phys. Rev. Lett. **94**, 113201 (2005).
[23] J. U. Andersen, E. Bonderup, and K. Hansen, J. Phys. B **35**, R1–R30 (2002).
[24] J. Szczepanski, S. Ekern, and M. Vala, J. Phys. Chem. A **101**, 1841 (1997).
[25] M. Vala, T. M. Chandrasekhar, J. Szczepanski, R. van Zee, and W. Weltner, Jr., J. Chem. Phys. **90**, 595 (1989).
[26] J. M. L. Martin, J. P. François, and R. Gijbela, J. Chem. Phys. **90**, 3403 (1989).
[27] N. Moazzen-Ahmadi, A. R. W. McKellar, and T. Amano, Chem. Phys. Lett. **157**, 1 (1989).
[28] N. Moazzen-Ahmadi, A. R. W. McKellar, and T. Amano, J. Chem. Phys. **91**, 2140 (1989).
[29] D. W. Arnold, S. E. Bradforth, T. N. Kitsopoulos, and D. M. Neumark, J. Chem. Phys. **95**, 8753 (1991).
[30] G. von Helden, P. R. Kemper, N. G. Gotts, and M. T. Bowers, Science **259**, 1300 (1993).
[31] S. Yang, K. J. Taylor, M. J. Craycraft, J. Conceicao, C. L. Pettiette, O. Cheshnovsky, and R. E. Smalley, Chem. Phys. Lett. **144**, 431 (1988).
[32] T. N. Kitsopoulos, C. J. Chick, Y. Zhao, and D. M. Neumark, J. Chem. Phys. **95**, 5479 (1991).
[33] P. Fuentealba, Phys. Rev. A **58**, 4232 (1998).
[34] M. W. Froese, K. Blaum, F. Fellenberger, M. Grieser, M. Lange, F. Laux, S. Menk, D. A. Orlov, R. Repnow, T. Sieber, Y. Toker, R. von Hahn, and A. Wolf, Phys. Rev. A **83**, 023202 (2011).
[35] J. U. Andersen, C. Brink, P. Hvelplund, M. O. Larsson, and H. Shen, Z. Phys. **40**, 365 (1997).
[36] A. Naaman, K. G. Bhushan, H. B. Pedersen, N. Altstein, O. Heber, M. L. Rappaport, R. Moalem, and D. Zajfman, J. Chem. Phys. **113**, 4662 (2000).
[37] J. B. Wills, F. Pagliarulo, B. Baguenard, F. Lépine, and C. Bordas, Chem. Phys. Lett. **390**, 145 (2004).
[38] M. Goto, J. Matsumoto, H. Shiromaru, Y. Achiba, T. Majima, H. Tanuma, and T. Azuma, Phys. Rev. A **87**, 033406 (2013).